Journal of Achievements in Materials and Manufacturing Engineering
VOLUME 39
ISSUE 1
March
2010

A study on the CO_2 laser welding characteristics of high strength steel up to 1500 MPa for automotive application

C.-H. Kim [a,*], J.-K. Choi [b], M.-J. Kang [a], Y.-D. Park [c]
[a] Korea Institute of Industrial Technology,
1-47 Songdodong, Yeonsugu, Incheon, South Korea
[b] Hyundai Rotem, 85, Daewondong, Changwon, Kyungsangnamdo, South Korea
[c] Dong Eui University, 995 Eomgwano, Busanjin-gu, Busan, South Korea
* Corresponding author: E-mail address: chkim@kitech.re.kr

Received 12.01.2010; published in revised form 01.03.2010

Manufacturing and processing

ABSTRACT

Purpose: This paper presents the mechanical and metallurgical characteristics of laser weldments for automotive steels with high strength ranging from 370 MPa to 1500 MPa.
Design/methodology/approach: Butt joint welding was conducted on high strength steel sheets by using a CO_2 laser with 6 kW output power. For sound welds with full penetration, the proper welding conditions were chosen and the cross-sectional bead shape, tensile strength, hardness profile and micro-structure were evaluated for each case.
Findings: Laser welding is known to be a low heat input process because of its high heat density and welding speed. But for laser welding of ultra high strength steel with strength over 780 MPa, micro-structural softening was observed in the HAZ (heat affected zone), resulting from dissolved martensite.
Practical implications: The tensile strength reduction in laser welding of ultra high strength steed should be considered in the design of car body structures. The HAZ softening that occurs in butt joint welding can reduce the tensile shear strength for overlap joint welds, which are predominantly mostly used in the BIW (body-in-white) structure.
Originality/value: This paper quantitatively demonstrates the occurrence of HAZ softening and a tensile strength reduction in laser welding of automotive steel with 780 MPa strength and more.
Keywords: Laser welding; Automotive; High strength steel; HAZ softening

Reference to this paper should be given in the following way:
C.-H. Kim, J.-K. Choi, M.-J. Kang, Y.-D. Park, A study on the CO_2 laser welding characteristics of high strength steel up to 1500 MPa for automotive application, Journal of Achievements in Materials and Manufacturing Engineering 39/1 (2010) 79-86.

1. Introduction

The automotive industry is continuously striving to develop light weight vehicles to address global warming. For light weight vehicles, the focus on materials is shifting increasingly from conventional steel to more advanced materials such as high strength steel, aluminum alloy, and reinforced plastic. Among the advanced materials, high strength steel, with advantages in cost and strength, ensures collision safety and is thus the most preferred material overall. Because high strength steel generally has less favourable formability, the application and use of dual phase (DP) steel, transformation induced plasticity (TRIP) steel, complex phase (CP), martensitic steel, and boron steel, which offer both strength and formability, is steadily on the rise [1-5].

For welding vehicle BIW, resistance spot welding has mainly applied been thus far, but with the development of new steel materials and evolution of welding technology of late, new joining techniques are being studied. Laser-based welding is applied to dissimilar materials and materials with dissimilar thickness like tailor welded blanks (TWB) [3-6]. In addition, with recent evolution of laser technology, various lasers are being applied to welding [7-13].

This study aims to perform butt joint welding on steel materials with strength between 370 MPa and 1500 MPa using a CO_2 laser and to investigate laser welding characteristics for each material type.

2. Experimental setup

In order to implement laser welding, a CO_2 laser was perpendicularly irradiated on the base material, as shown in Fig. 1. Here, the focal distance was 250 mm, and the focus was on the base metal surface, while the laser output power was 6 kW. Helium was used as a shielding gas and was supplied at 20 1/min through a gas nozzle.

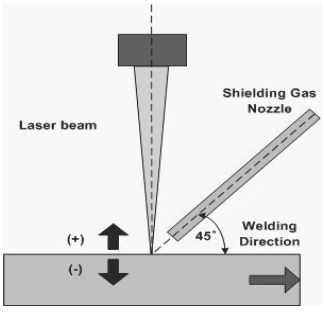

Fig. 1. Schematic diagram of experiment

As shown in Table 1, butt welding was performed by using steel sheets whose tensile strength is between 370 MPa and 1500 MPa. SAPH steel, which is a hot rolled steel, had relatively low strength, between 370 MPa and 440 MPa, compared to other steel materials used in this experiment, and its thickness was 1.8 mm. As for DP and TRIP steels, materials having strength of 590 MPa and 780 MPa, respectively, were used. In terms of CP steel consisting of various phases, 1180 MPa sheets were used, while the strength of Usibor™ steel, a kind of hot stamping steel, was enhanced to 1500 Mpa after undergoing hot stamping, owing to the addition of boron. Welding speeds enabling full penetration were set depending on each material's thickness, and butt welding was conducted.

Table 1.
Thickness and welding speed for each material

Material	Thickness (mm)	Welding speed (m/min)
SAPH370	1.8	6
SAPH440	1.8	6
DP590	1.4	7
TRIP590	1.4	7
DP780	1.8	6
CP1180	1.2	9
Usibor	1.6	6

After butt welding, each specimen was checked for weld defects, such as porosity on the weldments, through an X-ray transmission test, and then a tensile strength test was performed. The outcomes of the X-ray transmission test and tensile strength test after welding each material are shown in Fig. 2 and Table 2, respectively.

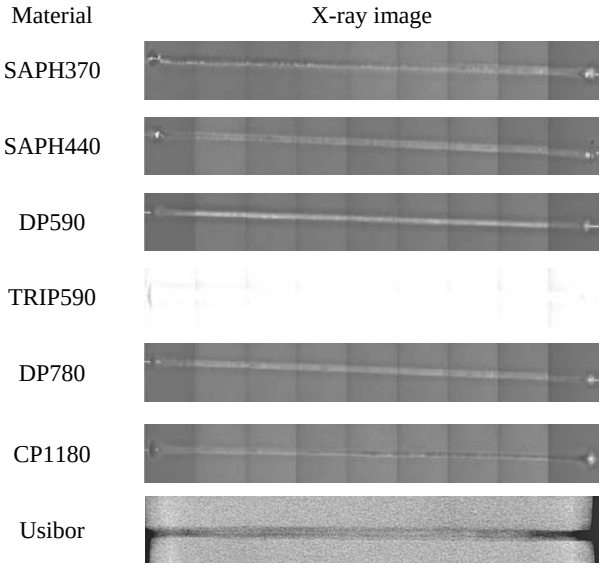

Fig. 2. X-ray transmitted images of weldments

Table 2.
Tensile test results

Material	Tensile strength (MPa)		Failure location
	Base metal	Weld-ment	
SAPH370	356	338	Base metal
SAPH440	420	424.8	Base metal
DP590	631	640	Base metal
TRIP590	672	670	Base metal
DP780	822	852	Base metal
CP1180	1230	1192	HAZ
Usibor	1522	1291	HAZ

Micro hardness profile was measured by applying a load of 200 g and by using a micro Vickers hardness tester. For the base material (BM), the heat affected zone (HAZ), and weld metal (WM), microstructure was observed by using an optical microscope, and a SEM analysis was performed on major weldments.

3. Hot-rolled steel, SAPH 370 and 440

Laser welding was performed on SAPH 370 and SAPH440 sheets with relatively low strength. The resulting bead shapes are shown in Fig. 3 and the hardness profiles are presented in Fig. 4. It can be confirmed that the hardness of the weld metal increased compared to the base material, and the microstructures of the two specimens at the base material, HAZ, and weld metal are shown in Fig. 5 and Fig. 6, respectively. SAPH440 had more alloy properties than SAPH 370, and thus has finer grains, but it generally displays similar tendencies. As for the base metal, its matrix phase consists of ferrite, and pearlite is observed partially at the grain boundary. At the HAZ, partial or full transformation from ferrite to austenite occurs depending on the area due to the heat generated using laser welding, and the structure shows a mixture of martensite and ferrite owing to rapid cooling. As for SAPH 370 steel sheet weld metal, grain boundary ferrite (GF) is found in large quantities as it goes through cooling after melting, and contains some bainite. The weld metal hardness, presented in Fig. 4, is roughly 230 HV, indicating that hardenability was not great depending on low alloying elements even at a high cooling rate of laser welding. The martensite structure found in the weld metal elevates the hardness of the weld metal. In contrast, the weld metal microstructure of the SAPH440 steel sheet consists of a mixture of martensite and bainite, which is attributable to an increase in alloying elements containing high hardenability, and its hardness level was elevated to 370 HV.

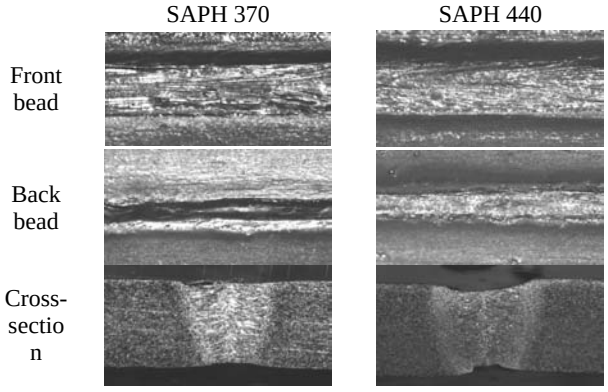

Fig. 3. Weld bead shapes for hot-rolled steel

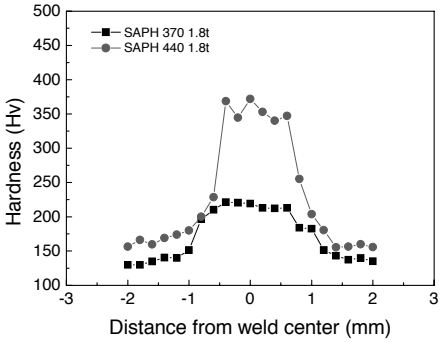

Fig. 4. Hardness profiles for hot-rolled steel

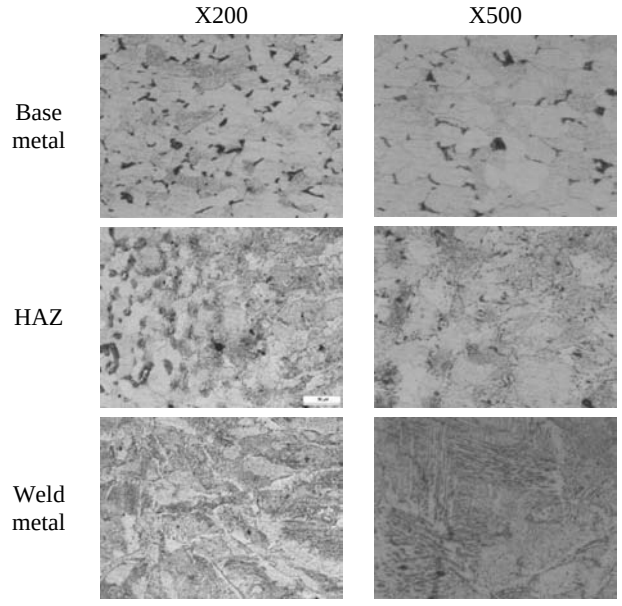

Fig. 5. Microstructures for hot-rolled steel, SAPH 370

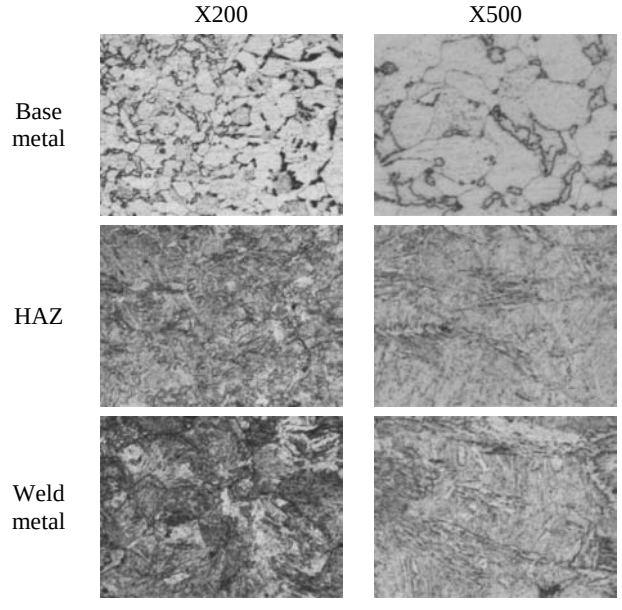

Fig. 6. Microstructures for hot-rolled steel, SAPH 440

4. DP 590 and TRIP 590 steel

Fig. 7 presents laser welding bead shapes of DP590 with 590 MPa strength and TRIP 590 steel, and the hardness distribution is shown in Fig. 8. As shown in Fig. 9, the DP 590 steel has a ferrite matrix phase and forms a dual phase with martensite found alongside the boundary. However, if the influence of heat extends beyond the A1 transformation point partially, as in the second point, the hardness level of the HAZ eventually increases as the ferrite matrix phase is transformed into austenite, leading to formation of a final structure consisting of martensite or bainite after cooling. Points 3 and 4, where there is greater heat influence, are heated over the austenite transformation temperature and then rapidly cool down, and thus mostly martensite structure is found. At Point 3, the maximum heating temperature ranges from 900° to 1100°, showing fine structure. As for the weld metal, only a martensite structure is observed, with no DP steel properties.

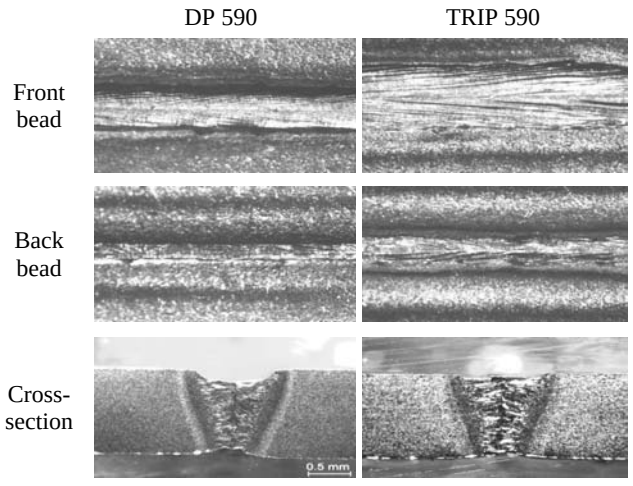

Fig. 7. Weld bead shapes for DP 590 and TRIP 590 steel

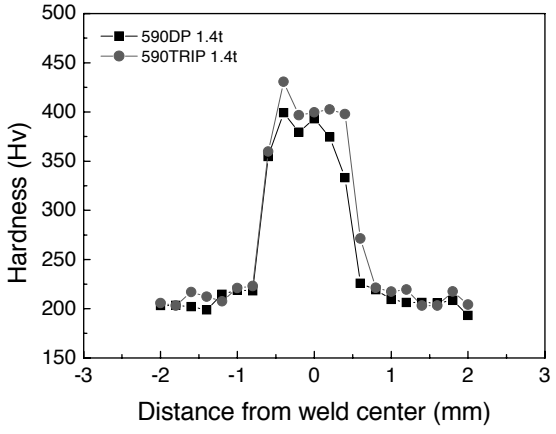

Fig. 8. Hardness profiles for DP 590 and TRIP 590 steel

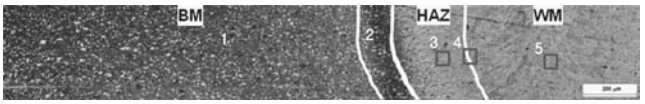

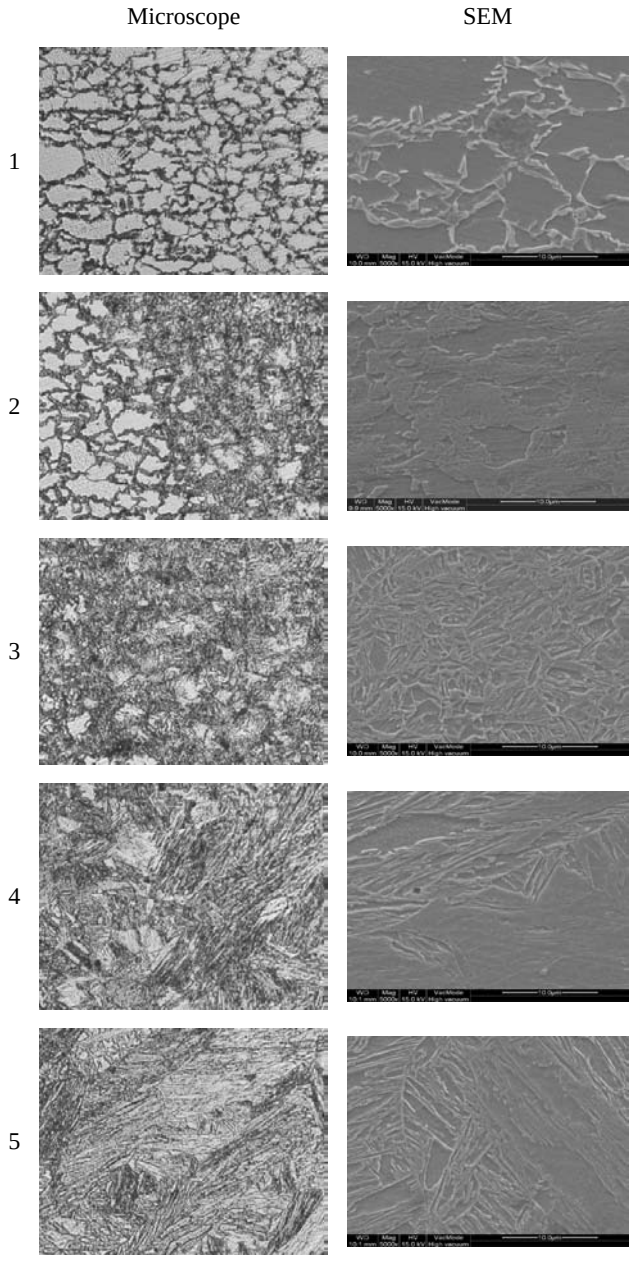

Fig. 9. Microstructures and SEM images for DP 590 steel

As can be confirmed in Fig. 10, the TRIP 590 steel's matrix phase is ferrite, which is similar to DP, and bainite is distributed at the boundary in a chain shape, while some retained austenite and martensite are observed at the boundary. The volume fraction of ferrite decreases from Point 2 where heat is applied, and

it consists mostly of bainite, and Points 3 and 4, where the influencing heat exceeds austerity's transformation temperature (Ac1). The weld metal that is heated beyond the melting temperature showed formation of mostly hard martensite structure, similar to the DP steel [14, 15].

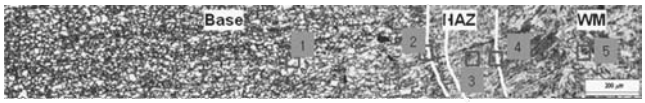

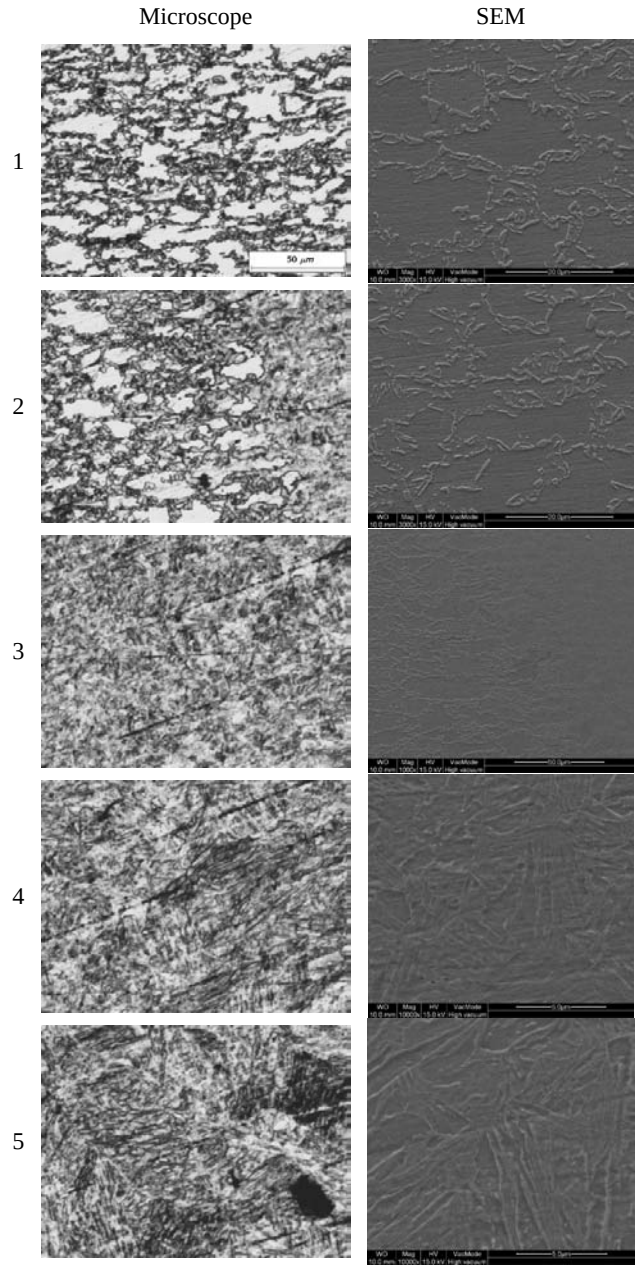

Fig. 10. Microstructures and SEM images for TRIP 590 steel

5. DP 780 and CP 1180 steel

Fig. 11 and Fig. 1 show the shape of laser weldments and hardness distribution with DP780 steel and CP 1180 steel. Compared to the aforementioned 590 MPa-level steel sheets, they are characterized by clear softening caused by a decrease in hardness at the HAZ. As can be confirmed in Fig. 13, the DP 780 steel forms a similar structure to that of the DP 590 steel, and it has a large amount of martensite volume fraction, while the grain size of the matrix ferrite size is finer. Comparison of SEM images at Points 1, 2, and 3 suggests that the maximum heating temperature at Points 2 and 3 almost reaches the critical temperature (Ac1), leading to a tempering effect. Therefore, HAZ softening occurs as martensite particles decompose and form tempered martensite. In other words, as the amount of martensite in the base metal increases, HAZ softening caused by martensite's decomposition intensifies. Although a martensite structure is formed at the weld metal, the structure is fine, because it has a rich alloying composition compared to the DP 590 steel. This also leads to higher weld metal hardness than the DP 590 steel.

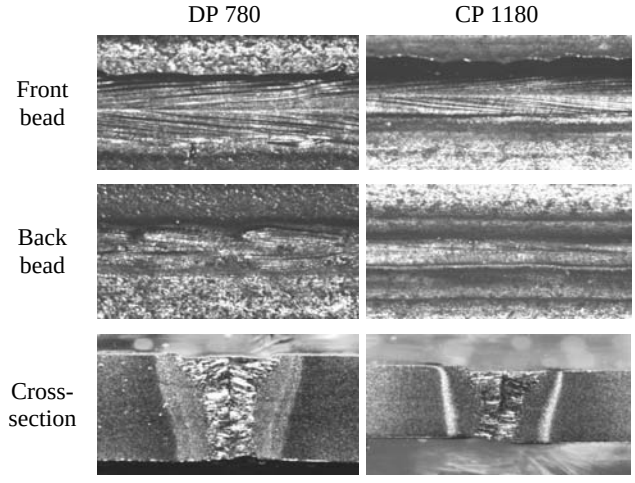

Fig. 11. Weld bead shapes for DP 780 and CP 1180 steel

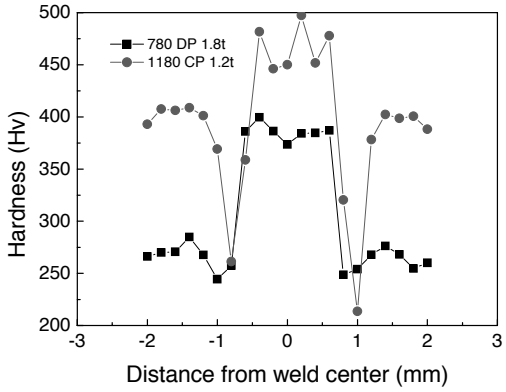

Fig. 12. Hardness profiles for DP 780 and CP 1180 steel

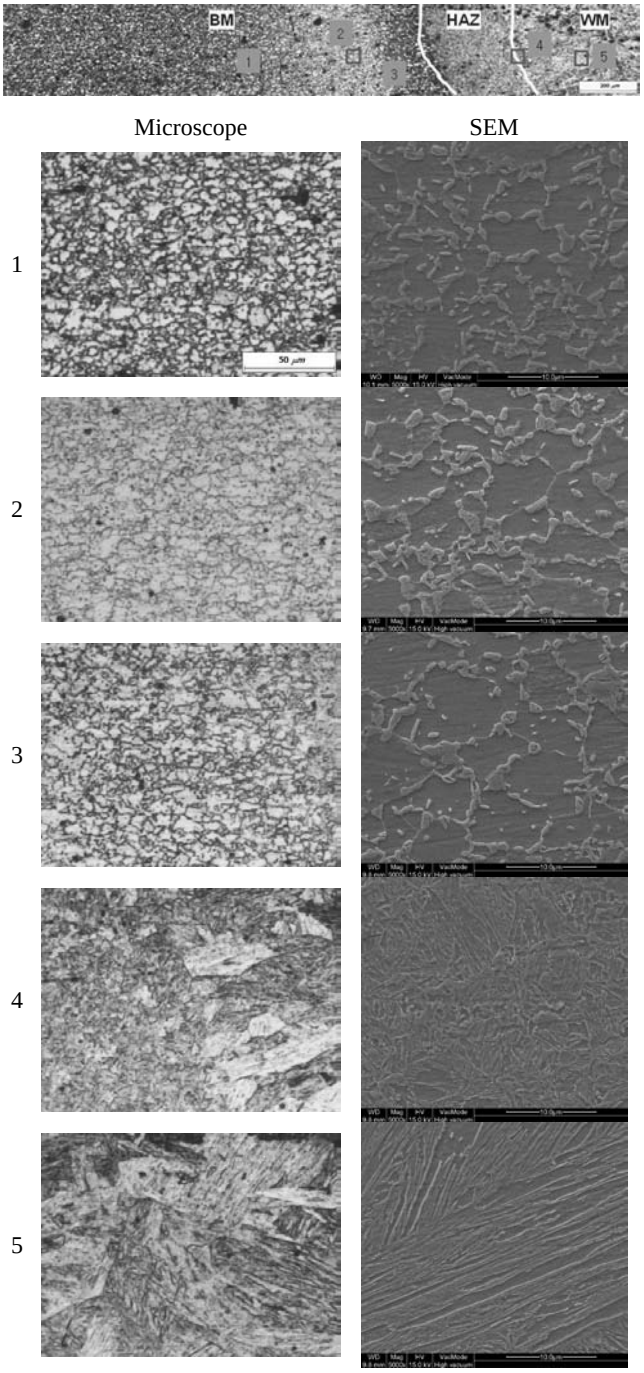

Fig. 13. Microstructures and SEM images for DP 780 steel

Meanwhile, CP steel has more than two phases, and can achieve higher strength, as it has characteristics of both TRIP steel and DP steel. As shown in Fig. 14, the base metal for the CP 1180 steel has various phases, high martensite content, and a structure with a fine yet highly complicated morphology of martensite phase. Due to the influence of heat, change in morphology of the martensite phase is observed from Point 2 (sub-critical HAZ), while at Point 3 the complex sub-morphology of martensite phase is largely absent. Therefore, it is predicted that this change is related to HAZ softening of the CP steel. However, the structure at Point 4, where it is heated beyond the austenite transformation temperature, is formed in a similar manner as in DP steel.

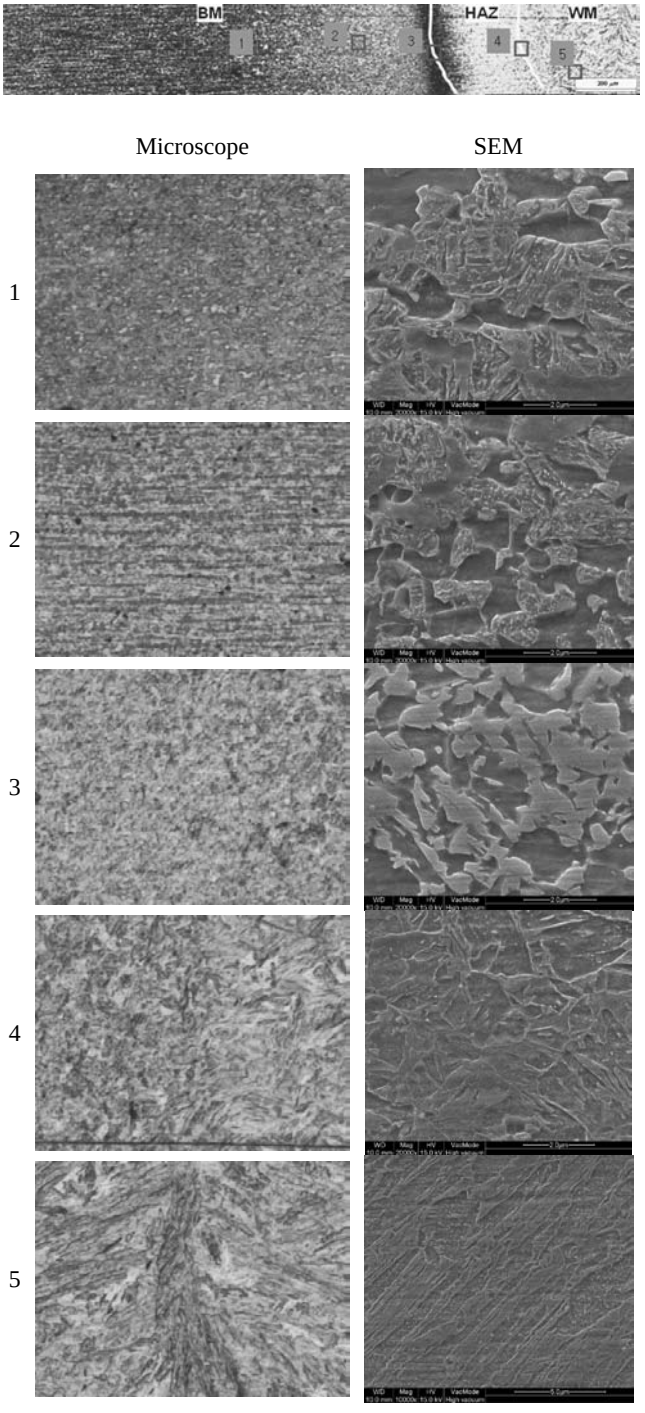

Fig. 14. Microstructures and SEM images for CP 1180 steel

6. Usibor™ steel

Usibor™ steel is a boron-alloyed steel whose strength is reinforced by using a hot stamping process. Its strength is between 500 MPa and 800 MPa prior to hot stamping, and ultimately surpasses 1500 MPa through martensitic quenching after heating at 900°. Fig. 15 shows the laser-welded cross section of Usibor™ steel, while Fig. 16 shows the hardness distribution. The hardness is the highest at the base metal and the weld metal, but degradation of hardness was most prominent at the HAZ.

As Usibor™ steel undergoes a martensitic quenching process, its base metal consists of martensite, as can be confirmed in Fig. 17. However, its structure is mixed with ferrite and martensite, because martensite transforms into tempered martensite or ferrite at HAZ, and this can be confirmed most clearly at Point 3.

Due to this, HAZ fracture, instead of base metal fracture, occurs during the tensile strength test, as shown in Table 2, and the tensile strength is 85% of that of the base metal.

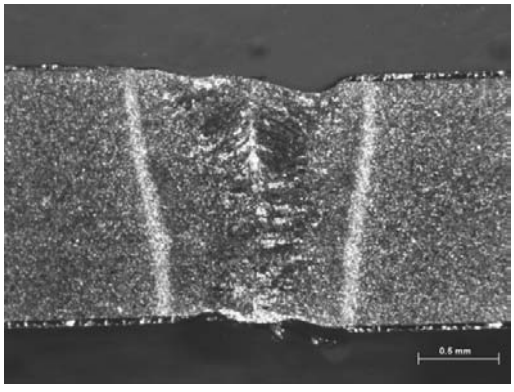

Fig. 15. Weld bead shape for Usibor steel

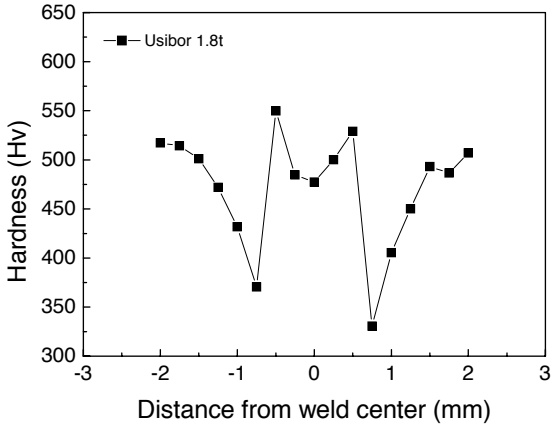

Fig. 16. Hardness profiles for Usibor steel

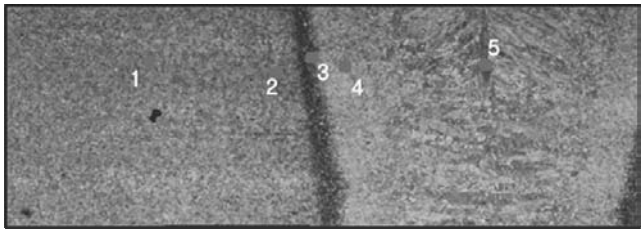

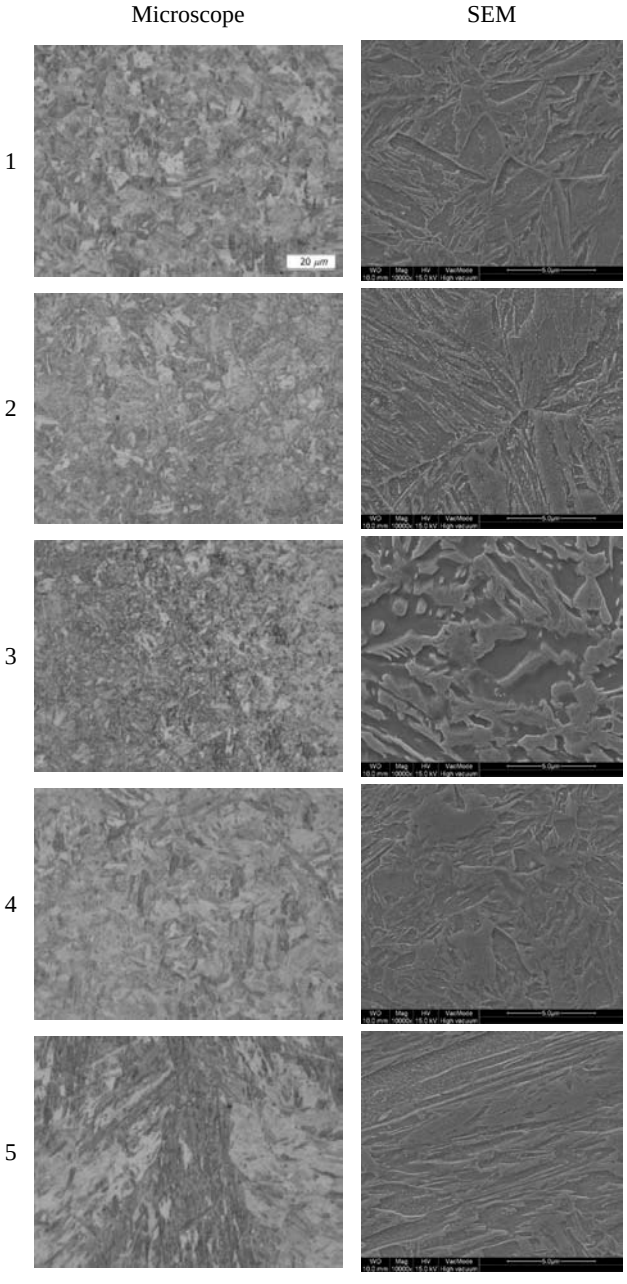

Fig. 17. Microstructures and SEM images for Usibor steel

7. Conclusions

In this study, laser welding was performed on steel plates with strength between 370 MPa and 1500 MPa and their welding characteristics were assessed. For steel materials with strength exceeding 590 MPa and whose base material has a martensite phase, a structure with lower hardness is found, as martensite undergoes decomposition at HAZ. With steel material having strength of over 780 MPa, this can be confirmed on the basis of the hardness distribution. As the amount of martensite at the base material increases, the tensile strength of steel material with strength exceeding 1180 MPa declines, and HAZ fracture rather than base material fracture takes place. Weldments of 1500 MPa-level steel material have as much as 85% of the base material's tensile strength. This softening of the HAZ occurs inevitably even when the heat input is reduced, and thus the strength degradation must be deterred by reducing the HAZ width by cooling it as rapidly as possible.

Acknowledgements

The authors would like to express their gratitude to Mr. W.-H. Choi in Shinyoung Ltd. and Dr. D.-C. Kim for their interests in this work and for supplying the specimens. Also the authors wish to thank Mr. S.-M. Lee and Mr. J.-W. Sohn of DongEui University for their SEM work support. Helpful discussions with Dr. W.-B. Lee are greatly acknowledged.

References

[1] R.R.G.M. Pieters, M.Y. Krasnoperov, I.M. Richardson, Laser welding of high strength steels, Proceedings of the 22nd International Congress „Applications of Lasers and Electro-Optics" ICALEO 2003, Jacksonville, Florida, US, 2003, 294-303.

[2] Z. Liu, M. Kutsuna, G. Xu, Fiber laser welding of 780 MPa high strength steel, Proceedings of the 25th International Congress „Applications of Lasers and Electro-Optics" ICALEO 2006, Scottsdale, Arizona, US, 2006, 562-568.

[3] S.G. Shi, S. Westgate, Fiber-delivered laser welding of ultra-high strength steels for automotive applications, TWI Report, The Welding Institute, 2007, Report No. 865/2007.

[4] C.M. Allen, Twin spot laser welding for dissimilar thickness steel tailored blanks, TWI Report, The Welding Institute, 2004, Report No. 793/2004.

[5] C.Y. Kang, T.K. Han, B.K. Lee, G.G. Chin, Hardness of laser welded AHSS with a strength over 600 MPa for automotive, Proceedings of 4th International Congress „Laser Advanced Materials Processing" LAMP 2006, Kyoto, Japan, 2006, Paper No. 06-276.

[6] W. Ehling, L. Cretteur, A. Pic, R. Vierstraete, Q. Yin, Development of a Laser Decoating Process for Fully Functional Al-Si Coated Press Hardened Steel Laser Welded Blank Solutions, Proceedings of 5th International WLT Conference „Lasers in Manufacturing" LIM 2009, Munich, Germany, 2009, 409-413.

[7] A. Russ, W. Gref, M. Leimser, F. Dausinger, H. Huegel, High speed welding of metal sheets with thin disk laser, Proceedings of 2nd International WLT Conference „Lasers in Manufacturing" LIM 2003, Munich, Germany, 2003, 229-234.

[8] G. Verhaeghe, P. Hilton, Battle of sources – using a high-power Yb-fiber laser for welding steel and aluminium, Proceedings of 3rd International WLT Conference „Lasers in Manufacturing" LIM 2005, Munich, Germany, 2005, 33-38.

[9] E. Beyer, B. Brenner, A. Klotzbach, S. Nowotny, Laser macro processing – today and tomorrow, Proceedings of 4th International Congress „Laser Advanced Materials Processing" LAMP 2006, Kyoto, Japan, 2006.

[10] F. Abt, F. Dausinger, Focusing of high power single mode laser beams, Proceedings of 4th International WLT Conference „Lasers in Manufacturing" LIM 2007, Munich, Germany, 2007, 321-324.

[11] J.-K. Kim, H.-S. Lim, J.-H. Cho, C.-H. Kim, Bead-on-plate weldability of Al 5052 alloy using a disk laser, Journal of Achievements in Materials and Manufacturing Engineering 28/2 (2008) 187–190.

[12] J.-K. Kim, H.-S. Lim, J.-H. Cho, C.-H. Kim, Weldability during the laser lap welding of Al 5052 sheets, Archives of Materials Science and Engineering 31/2 (2008) 113-116.

[13] C.-H. Kim, H.-S. Lim, J.-K. Kim, Position welding using disk laser-GMA hybrid welding, Journal of Achievements in Materials and Manufacturing Engineering 28/1 (2008) 83-86.

[14] M.S. Xia, M.L. Kunts, Z.L. Tian, Y. Zhou, Failure study on laser welds of dual phase steel in formability testing, Science and Technology of Welding and Joining 13 (2008) 378-386.

[15] M. Xia, E. Biro, Z. Tian, Y.N. Zhou, Effects of heat input and martensite on HAZ softening in laser welding of dual phase steel, ISIJ International 48 (2008) 809-814.